CASL-U-2014-0188-000

Power uprates
and plant life extension

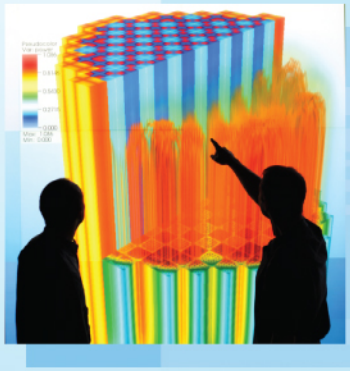

Engineering design
and analysis

Science-enabling
high performance
computing

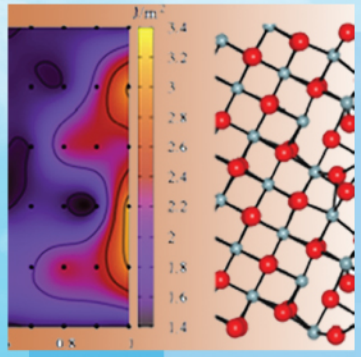

Fundamental science

Plant operational data

Consortium for Advanced Simulation of LWRs

L3:PHI.VCS.P9.01

Development of CTF Capability for Modeling Reactor Operating Cycles with Crud Growth

Robert Salko

Oak Ridge National Laboratory

September 30, 2014

U.S. DEPARTMENT OF ENERGY | Nuclear Energy

CASL-U-2014-0188-000

Development of CTF Capability for Modeling Reactor Operating Cycles with Crud Growth

Milestone: L3.PHI.VCS.P9.01
Document: CASL-U-2014-0188-000

Bob Salko*
(865) 576-5339
salkork@ornl.gov

Travis Lange†
tlange@vols.utk.edu

Scott Palmtag‡
(910) 620-6540
scott.palmtag@corephysics.com

Jess Gehin§
(865) 576-5093
gehinjc@ornl.gov

September 30, 2014

Abstract

CTF is a thermal-hydraulics simulation tool designed for modeling both fluid and solid regions inside light water reactor vessels. It forms the thermal-hydraulic package of the Virtual Environment for Reactor Applications Core Simulator being developed by the Consortium for Advanced Simulation of Light water reactors. The project documented by this report has been undertaken to add a new crud-modeling capability to CTF. Achieving this goal required the completion of three specific tasks: (1) developing a method for running CTF simulations of reactor operating cycles , (2) developing and implementing a basic crud modeling "surrogate", and (3) developing and implementing a method for inputting detailed core power distributions. These three tasks have been completed and have resulted in a new feature that allows users to run long-time-scale simulations with CTF as a collection of individual, steady-state points that comprise a larger transient. The user is able to drive inlet mass flow rate, inlet temperature, outlet pressure, and core power distributions to new values for each state in the simulation. The crud modeling tool is used at each of these state points to grow crud as a function of current thermal hydraulic conditions of the previously solved state. The developed crud modeling tool makes many simplifications that allow it to make

*Oak Ridge National Laboratory
†University of Tennessee
‡Core Physics
§Oak Ridge National Laboratory

a crude approximation of general crud behavior. It is envisioned that the infrastructure that has resulted from this project will be utilized in the future to facilitate coupling to more advanced crud chemistry codes. This document details work completed during this project and demonstrates the verification of this new capability.

Acknowledgements: This work has been supported by the Consortium for Advanced Simulation of Light Water Reactors (www.casl.gov), an Energy Innovation Hub for Modeling and Simulation of Nuclear Reactors under U.S. Department of Energy Contract No. DE-AC05-00OR22725.

1 Introduction

The formation of Chalk River Unidentified Deposits (crud) on nuclear fuel rods has been a long-standing problem in the commercial nuclear power industry [1]. Because of the operational and economic impacts of crud deposition, it is important to have a thorough understanding of its behavior. crud deposition will manifest itself as two primary phenomena: Crud-Induced Power Shift (CIPS) and Crud-Induced Localized Corrosion (CILC). CIPS is caused by boron being absorbed into the porous crud layer and then locally depressing the neutron flux at those absorption points. Since crud will generally form in the upper portion of the core, the core power will shift to the bottom of the core, forcing the reactor to be operated at reduced powers to stay within safety guidelines. The CILC phenomena can lead to fuel rod failure. While the failure mechanism is not known with certainty, it is believed that, as crud forms, a vapor blanket develops and impedes heat transfer from the cladding surface, causing temperature rise, corrosion acceleration, and ultimately, cladding failure [2].

The CTF code [3] is the subchannel thermal hydraulic capability being used in Virtual Environment for Reactor Applications (VERA)[1] in the Consortium for Advanced Simulation of Light water reactors (CASL) program[2]. The primary functions of the code are solving for the fuel rods, unheated conductors, and coolant behavior in the reactor. It solves a 9-equation model, which makes it suitable for two-phase flow modeling and especially accident scenarios.

The primary goal of this project was to add a crud-modeling capability to CTF. Specifically, we wanted to model crud deposits on the nuclear fuel rods over long transients (i.e. reactor operation cycles). Not only did we look to capture the effect of the thermal hydraulic solution on crud growth but, reciprocally, we also wanted to capture the effects of the crud layer on the thermal hydraulic solution. This goal required the completion of several subtasks.

CTF already does a transient solution, but the physics it was developed to solve necessitate a highly resolved time scale (e.g. 1×10^{-6} to 0.1 second timesteps). This makes doing the long-time-scale simulations noted above impractical from a computational standpoint. Therefore it was necessary to de-

[1] Best reference for this?
[2] Reference a document or the website?

CASL-U-2014-0188-000

velop a capability in CTF for modeling long transients with very coarse timestep sizes.

This task was achieved by modeling the operational cycle as a string of steady-state solves, each solve using the results of the previous core state as the starting guess for the next state. This approach required dividing the CTF solution process into individual components (e.g. model read-in and initialization, steady-state solve, results writing) and then orchestrating those individual tasks using an external driver program.

In addition to simply executing the solution steps, it was also necessary for the driver to be able to access data in CTF for modification of simulation boundary conditions as well as new crud solution data. This communication was primarily achieved via a newly developed coupling interface to CTF that has proven useful in both simplifying coupling to CTF as well as protecting its internal data.

The CTF driver is capable of setting new values for core inlet flow, core outlet pressure, and core inlet temperature at each state point. An additional feature was added to specify a new detailed core power distribution via an external Hierarchal Data Format 5 (HDF5) file. With these added capabilities, the CTF driver made it possible to model months and years of reactor operation.

To capture the crud growth behavior over reactor operation periods, a basic crud modeling "surrogate" was developed. In this step, we did not set out to create a highly accurate crud modeling tool; rather, the surrogate was designed to capture the general behavior of crud growth with respect to thermal hydraulic conditions. That is, it was designed to take reactor operation time, model size, and the core boiling distribution as inputs, making simplifying assumptions about coolant chemistry, crud composition, and material properties.

To complete the task of adding crud modeling in Pennsylvania State University version of COBRA-TF (CTF), the crud layer was added to the CTF fuel rod conduction equation. This allows the increased thermal resistance of the crud layer to be felt in locations having deposits. This step primarily involved adding an additional node (thermal resistance) to the fuel rod radial conduction equation.

2 CTF Driver

Development of an external driver program was necessary to do a string of CTF state solves, set state operating conditions, and run the crud surrogate. This driver represents the infrastructure that enabled us to implement the reactor cycle and crud modeling capability into CTF. As a precursor to developing this driver program, an explicit coupling interface was developed for CTF.

This interface sections the code into separate pieces (e.g. initialize the code, run a steady-state simulation, write output, change boundary conditions, read an HDF5 power distribution file, etc.). The actual implementation of the interface is a module in the CTF source directory that groups together many procedures capable of accessing internal CTF data and calling internal CTF

procedures. This coupling interface module provides many benefits to both CTF and the coupled code, including:

- providing coupled codes a means for controlling different steps in the CTF simulation process,
- offering procedures for passing thermal hydraulic solution data out of CTF,
- offering procedures for setting boundary conditions in CTF (inlet flow, inlet temperature, outlet pressure, power distribution),
- providing documentation on all procedures, making their usage straightforward while hiding the details of their implementation, and
- protecting internal CTF data from accidental mis-use.

The CTF driver was designed to use this coupling interface almost exclusively to drive the CTF state solves and modify CTF data. One exception is the modification of rod surface crud data; the CTF driver will directly access CTF surface objects to set attributes like crud thickness, conductivity, and mass. For the sake of consistency and good coding practice, access procedures should be added to the coupling interface to modify rod surface crud data.

The CTF driver is a separate utility, written in Fortran, that uses the CTF coupling interface to drive the CTF solution. The driver program was designed to take two optional arguments: (1) the name of the multi-state input file, and (2) the name of the CTF input file. The code is run as follows:

```
$CTF_DRIVER --state_file=<state_filename>.inp
--ctf_file=<ctf_filename>.inp
```

The multi-state input file is a plain text file that is used to turn the crud model on/off and to specify state point operating conditions. An example of a multi-state input file with 3 states in the solve is given in Figure 1. The first line in the figure turns on the crud modeling if set to 1. The second line declares the number of states to be modeled. The following lines provide boundary conditions for each state; one line should be given for each of `num_states`. In these lines, the first column is the month, the second column is the total core inlet mass flow rate in kg/s, the third column is the inlet temperature in Celsius, and the fourth column is the core outlet pressure in MPa. If the CTF driver is run without the multi-state input file, it will default to doing a single CTF steady-state solve with no crud modeling.

The CTF input file is the traditional Pennsylvania State University version of COBRA-TF input deck that must be created as specified in the CTF User Manual [4]. This option allows the user to specify a custom name for the CTF input deck. Running the CTF driver without this option will default to looking for a CTF input file named `deck.inp`.

CASL-U-2014-0188-000

```
model_crud 1
num_states 3
0.0  0.3275943 292.7777778 15.51320390
3.0  0.3275943 292.7777778 15.51320390
6.0  0.3275943 292.7777778 15.51320390
```

Figure 1: Example of the multi-state input file

The design of CTF driver algorithm is presented as a flowchart in Figure 2. The initial steps are to read the multi-state input file and initialize CTF. The actual simulation is performed in a series of CTF solves (one for each state), which is represented by the loop in Figure 2. The boundary conditions specified in the multi-state input file and optional HDF5 power input file are set at the beginning of a state solve. A steady-state CTF solve is then done for the state to calculate the new resulting thermal-hydraulic profile in the core, using the previous state's solution as an initial guess. The crud surrogate is run after the steady state solve using the newly calculated thermal hydraulic solution. This newly deposited crud will impact rod thermal solution in the next state. To complete the state, the CTF driver directs CTF to write simulation data pertaining to that state as a new group in the output HDF5 file.

CASL-U-2014-0188-000

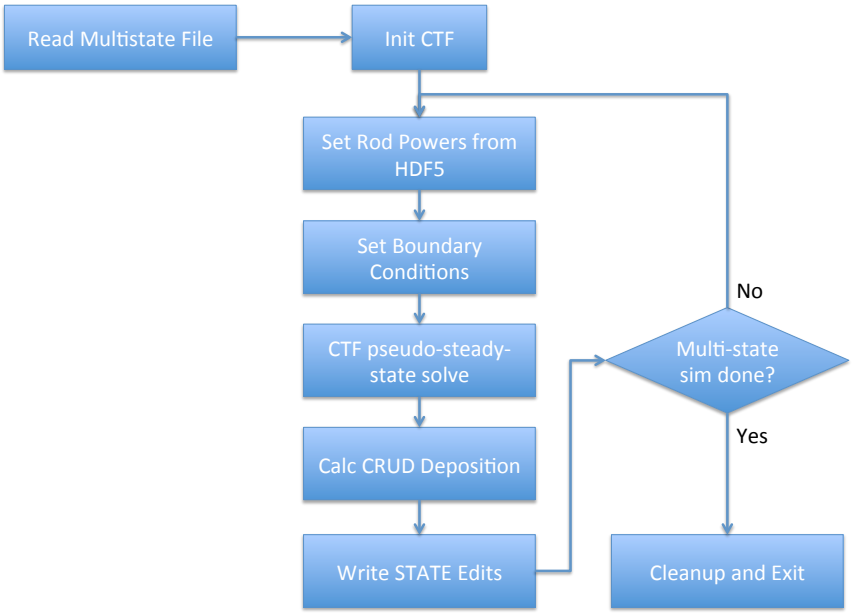

Figure 2: Flowchart of the multi-state driver created to drive CTF multi-state simulations

3 Power Distribution Input

The power distribution is given via a separate HDF5 file that organizes each core power profile into a separate group in the file. The groups are named using the convention "STATE_XXXX", where "XXXX" is a four digit number that represents the state number. The state number should run from 0001 to `num_states`.

In each state group, pin power is specified as required by the VERA HDF5 Output Specification [5]. Rod power is given as a 4-D array, with the indices being: (1) assembly ID, (2) axial level ID, (3) local row of rod in assembly, and (4) local column of rod in assembly. With this new rod power input capability, it is possible to input detailed power distributions in CTF.

It is possible to produce this file directly from CTF using one of the procedures in the CTF Coupling Interface module, as this feature also doubles as a simple restart function in CTF. The HDF5 power distribution file name should follow the convention `<name>.ctf.restart.in.h5`. A more beneficial option would be to produce a realistic power distribution in this file format from an external neutronics code and then use that for the cycle simulation that is run with the CTF driver.

4 Crud Surrogate Design

This task was to create a basic tool—a "surrogate"—that would capture the general behavior of crud growth on fuel rods. It was not envisioned that this preliminary development would be accurate for modeling real crud deposition but, rather, would serve as a utility for building the infrastructure necessary to couple to more robust crud chemistry codes in the future. With that said, the surrogate does live in the CTF repository and will be distributed with the code. Future activities may involve improving this simple capability by adding more physically accurate models and replacing many of the simplifying assumptions that have been made.

The work of Zou et al. [1] was used as a basis for the design of this surrogate. Since the local boiling rate is a strong driver for crud growth, the authors used this as the main variable in their crud deposition model shown in Equation 1.

$$D_i = \frac{q''_{b,i}}{q''_{b,\mathrm{tot}}} D_{\mathrm{tot}} \tag{1}$$

In the equation, D stands for the crud deposition rate and q''_b is the boiling rate. The subscripts "i" and "tot" represent the localized value and total, core-wide values, respectively. In the case of CTF, i represents the value for a single rod surface, which is defined as one level of one rod azimuthal segment, as shown in Figure 3. In the case of this crud surrogate, the units for the deposition rates were chosen to be in kg.

CTF is capable of providing the local and total core boiling rates, which leaves only the D_{tot} term of Equation 1 to be defined. This is done using the

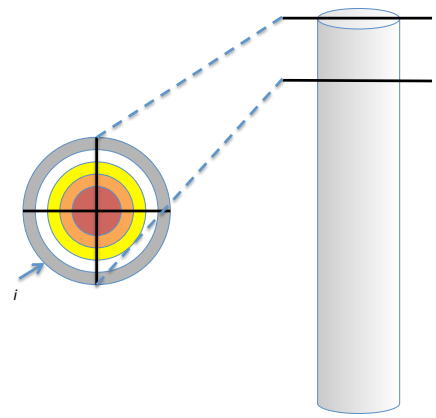

Figure 3: Diagram of CTF rod meshing (side view of rod on right, top view of axial cutaway of rod on left)

findings in the Electric Power Research Institute (EPRI) report produced by Sawochka [6]. The author indicated that crud deposition rates will be a function of coolant chemistry and, specifically, coolant impurities due to primary coolant system corrosion. They provided the balance equation shown here in Equation 2, which balances corrosion release and removal through the coolant purification system with impurity deposition on fuel rods and other primary coolant system surfaces.

$$\begin{aligned}&\text{Corrosion Release} - \text{Purification System Removal} = \\ &\text{Deposition on Fuel} - \text{Deposition Elsewhere}\end{aligned} \tag{2}$$

Based on experimental operating plant observations, the author presents the following corrosion rate correlations for Alloy 600 (Equation 3) and Stainless Steel (SS) (Equation 4), two of the primary construction materials in the primary coolant loop of Pressurized Water Reactor (PWR)s. Corrosion rate is given in mg/dm^2-month.

$$\mathrm{CR}_{600} = 1.6(10^6)[H^+] + 1.84 \tag{3}$$

$$\mathrm{CR}_{SS} = 3.4(10^6)[H^+] + 3.66 \tag{4}$$

Here, $[H^+]$ is the hydrogen ion content, which defines the acidity of the solution. It is assumed that this value is to be specified in units of mol/l, but this was not explicitly stated in the documentation. The value for $[H^+]$, in

mol/l, can be obtained using the relationship given in Equation 5. It is assumed, in the surrogate, that pH of the coolant is neutral at 7.0.

$$\mathrm{pH} = -\log_{10}[H^+] \tag{5}$$

While these correlations give the corrosion rate, it is actually the mineral release rate that will result in impurity mass being suspended in the coolant. The Release Rate (RR) is obtained by multiplying the corrosion rate by a multiplication factor, K_{SS} or K_{600}, as shown in Equations 6 and 7. The authors suggested this will vary between 0.1 and 0.5.

$$\mathrm{RR}_{600} = K_{600}\mathrm{CR}_{600} \tag{6}$$

$$\mathrm{RR}_{SS} = K_{SS}\mathrm{CR}_{SS} \tag{7}$$

The units of these two equation will be in mg/dm^2-month, but we look to find the total mass of impurities released into the coolant over a given operational period (the time between state points). To determine this, we need to multiply the result of these correlations by the total primary coolant system surface area as well as the length of the operational period. Table 4-1 of the EPRI paper provides total surface areas of different materials in some typical reactor types (i.e. Westinghouse 810 MW three-loop plant, Westinghouse 1095 MW four-loop plant, ABB-CE 860 MW two-loop plant, and B&W FA 177 Plant). The values in this table are useful for providing an approximation of corrodible area in a model, but need to be scaled for the individual problem being run by the crud surrogate. Therefore, the coolant system surface area for the Westinghouse 4-loop plant was implemented into the crud surrogate as a parameter with a scaling factor later applied. The scaling factor was based on the number of rods in the model assuming that the Westinghouse 4-loop plant has 60,000 rods. Therefore, the coolant system surface area of a model in CTF will be calculated using Equation 8.

$$A_{\mathrm{model}} = A_{\text{W-4}}\frac{n_{\mathrm{rods}}}{60,000} \tag{8}$$

In the equation, A_{model} is the surface area to be used in the crud surrogate, $A_{\text{W-4}}$ is the value given for a Westinghouse 4-loop plant in the EPRI report, and n_{rods} is the number of rods in the CTF model.

For the operational period, we simply take the difference between the month of the current state and the previous state. This gives us the total mass of impurities released between the two state points.

At this point, we can use Equation 2 to determine the amount of impurities that will be deposited in the core as crud. Lacking information on the purification system, we choose to simply neglect the system. The EPRI paper does give an example in which the purification system will remove 7–8% of impurities from the system, so this simplifying assumption should be reasonable. Additionally, since boiling is a major driver of crud deposition, we also assume that crud only

CASL-U-2014-0188-000

deposits on boiling surfaces, which eliminates the fourth term from Equation 2. This simply means that all corrosion products released into the coolant during an operational period will form the total deposition rate, D_{tot} of Equation 1.

By this process, we arrive at a local mass of crud deposited onto a fuel rod surface over a given operational period. In order to capture the feedback of this deposited crud in the fuel rod conduction equation, we need to also quantify its thickness. By assuming that the geometry is cylindrical and that the crud was deposited uniformly over the surface, we are able to calculate the crud volume using Equation 9.

$$V = \pi \left(r_o^2 - r_i^2\right) L \tag{9}$$

In this equation, V is the volume of the newly deposited crud on the fuel rod surface, r_o is the outside radius of the crud, r_i is the outside radius of the rod, including any previous crud deposits, at the beginning of the current operational period, and L is the axial height of the current surface segment being analyzed. By expressing V as crud mass over crud density, m/ρ, we can evaluate the new outside radius of the rod after the mass, m, of crud has been deposited as shown in Equation 10.

$$r_o = \sqrt{\frac{m}{\pi \rho L} + r_i^2} \tag{10}$$

This also requires, of course, that we have an estimate of crud density. Lacking a source for such a number, it was simply assumed that crud density is approximately equal to that of iron (7000 kg/m^3). After solving for r_o, we can calculate thickness increase due to deposited mass, m, by subtracting the initial rod radius, r_i, from this value.

A final component needed for solution of the fuel rod conduction equation is the crud thermal conductivity. For simplicity, it is taken as a constant 15 W/m-K.

The surrogate design that has just been detailed involved making several important assumptions which are summarized here:

1. The core pH is a neutral 7.0; decreasing this will result in more corrosion products being released and deposited on the fuel rods;

2. The release rate of corrosion products into the coolant is 50%;

3. There is no coolant system cleanup, so all corrosion products released in a given state period are deposited onto the nuclear fuel rods;

4. The total coolant inventory of dissolved impurities ends up on the fuel rods; in reality, there will be chemical reactions that will result in the actual deposited mass being different from this value;

5. The steaming rate is the only determining factor in where crud will deposit;

6. The coolant system surface areas provided for the Westinghouse 4-loop plant in the EPRI report [6] are used to determine corrosion product release and must be scaled for each individual problem assuming there are 60,000 rods in the 4-loop plant;

7. The crud density will have a large impact on predicted crud thickness; it was somewhat arbitrarily set to a density close to that of iron (7,000 kg/m^3). Likely, it will be much less than this.

8. A constant thermal conductivity and density of the crud was selected whereas, in reality, both of these terms should have a temperature dependence.

5 Crud Thermal Resistance

The previous section discussed the crud surrogate, which will result in a mass of crud being deposited on each rod surface that experiences some amount of boiling. This mass is converted into a thickness that is set in the rod surface data class in CTF. The purpose of the task discussed in this section is to capture the effect of the crud layer on thermal resistance at the surface of the fuel rod during the CTF rod conduction equation solution.

Figure 4 shows the radial nodalization of a nuclear fuel rod with the new crud layer added. In the figure, the red region represents the fuel pellet, the blue region is the clad, and the grey region is the crud layer. Note the placement of the nodes in the model; nodes in Rings 1 and 2 of the fuel pellet are at the mesh cell center, while all other nodes lie on object surfaces. So that the clad conduction equations result in temperatures at both surfaces, the clad region is divided into two mesh cells with the nodes lying on inside and outside surfaces. The crud layer is modeled as one single region with its node at its exterior surface. Therefore, the temperature distribution in the crud layer will be uniform and equal to its surface value. This is a good assumption considering the small thickness of the crud layer.

A few simplifying assumptions were made when implementing this feature into CTF:

1. there is no consideration made for axial or azimuthal conduction in the crud layer,

2. there is no heat generation in the crud layer,

3. the crud layer has no impact on clad oxidation or clad-water reaction heat generation, and

4. there is no thermal contact resistance between the clad and crud layer.

Furthermore, a conduction equation is added for the crud layer only if the crud thickness is above a minimum criterion of 0.1 microns. This results in

CASL-U-2014-0188-000

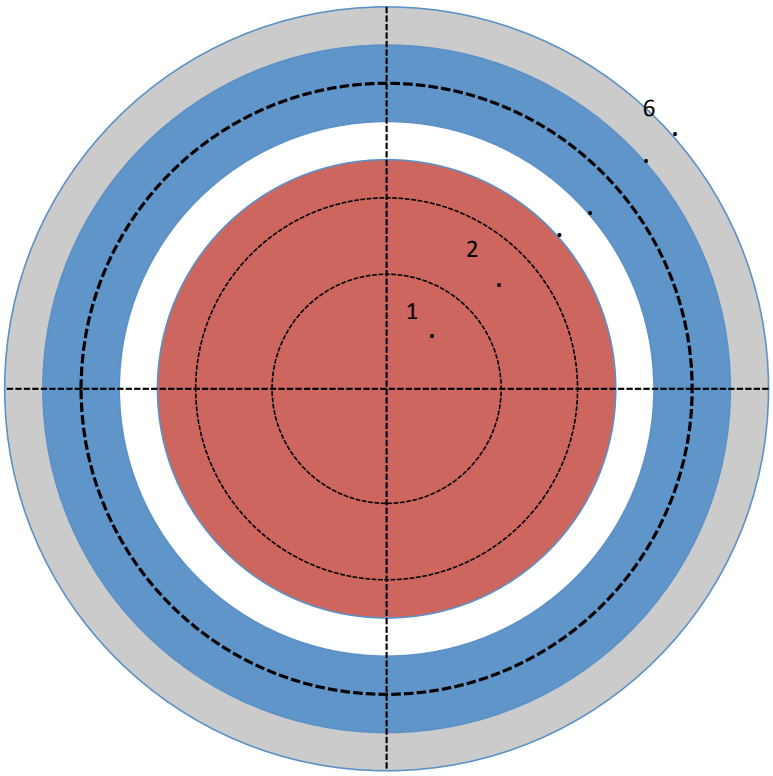

Figure 4: Radial noding of nuclear fuel rod with crud layer in CTF

no change to the original CTF rod solution for rods with very little to no crud present. This was done to prevent an unnecessary addition to the computational time. Despite this, all rod objects in the code are formed from a data structure that will have a node for the crud layer. Therefore, for rod surfaces with no crud, the fuel rod radial computational node representing the crud layer will have its temperature set to the solution for the clad outside surface.

The thermal conduction equation solved by CTF for an arbitrary solid mesh cell in Figure 4 is as follows:

$$\frac{d}{dt}\int_V \rho C_p V T = \oint_A \boldsymbol{n}_k Q_k dA + \int_V Q''' dV - \oint_A Q_s dA \tag{11}$$

The Left-Hand Side (LHS) term is the transient term, with ρ being material density, C_p being material specific heat, T being the material temperature, and t being the timestep size of the solid conduction equation solution. On the Right-Hand Side (RHS), the first term is a surface integral over the solid mesh cell that accounts for energy conduction in axial, azimuthal, and radial directions. The $\boldsymbol{n}$ is the unit vector orthogonal to the surface, k is the current surface, and A is the surface area of the solid mesh cell. The second term represents volumetric generation of energy due to fission or electrical heating with Q''' being the volumetric energy generation rate and V being the cell volume. The third, and final, term of the equation is the convective heat transfer at the cell surface which transports energy from the solid to surrounding fluid or vice versa. Note that only mesh cells exposed to the coolant will have this final term. Furthermore, only mesh cells having some heating source will have the volumetric energy generation term.

The CTF rod solution algorithm works by looping over each rod, then each axial level of the rod, then each azimuthal segment at that level. For a single segment, CTF then loops over each radial node and sets up the terms that will form the equation for that node. At the end of each radial node loop, the system of equations will be solved by Gaussian elimination. Therefore, the rod conduction solution is implicit in only the radial direction; azimuthal and axial conduction terms are added to the conduction equations explicitly.

In the CTF solution, the thermal conduction term, Q_k, will be expanded for each surface of the current cell being setup. Each conduction term will take on the form shown in Equation 12, where a represents the mesh cell being solved and b represents a connected mesh cell.

$$Q_{a\to b} = k_{ab}\left(T_b - T_a\right) \tag{12}$$

Note that the average thermal conductivity between Cell a and b will be some combination of the individual thermal conductivities of the two cells, k_a and k_b. This averaged thermal conductivity is defined using the concept of thermal resistances as shown in Equation 13, where $R_{a\to\text{boundary}}$ is the thermal resistance from the node of Cell a to the boundary between Cells a and b and $R_{\text{boundary}\to b}$ is the thermal resistance from the boundary to the node of Cell b.

CASL-U-2014-0188-000

$$k_{ab} = \frac{1}{R_{a\rightarrow\text{boundary}} + R_{\text{boundary}\rightarrow b}} \tag{13}$$

The thermal resistance for the radial direction will be that of a cylindrical geometry as shown in Equation 14.

$$R = \frac{\ln\left(\frac{r_o}{r_i}\right)}{2\pi k L} \tag{14}$$

Here, r_o and r_i are the outside and inside radii of the cylindrical mesh cell, k is the thermal conductivity, and L is the axial height of the cell. With the concept of thermal resistances introduced, the fuel rod system of equations can be posed in terms of a system of thermal resistances, presented in Figure 5 for a nuclear fuel rod. In this example, the fuel rod is broken into 6 mesh cell volumes, each with a node, labeled as N1–N6, that is either at the mesh cell center or surface. There are, as a result, 8 thermal resistances, labeled as R1–R8. Note that cells having a node at their center will have two thermal resistances; one to communicate with each cell boundary. Since the crud layer has only one node at its outside surface, it requires only one thermal resistance.

In the original CTF solution, when the code reached the clad outside node, it would add a thermal resistance of zero ($k = \infty$) for the conduction to the fluid. The convective heat transfer term would be added to the equation after the node loop was complete and prior to the solution of the system of equations. For this work, this algorithm was modified to check if there is crud during this radial node loop. If there is no crud, the equation system is setup as it was originally. There will still be a crud node if crud modeling is turned on; however, no equation will be setup for that node and, instead, the temperature of that node will be set to the clad outside temperature. On the other hand, if crud is present, the thermal resistance on the clad outside surface will be set to that of the crud and the zero resistance will be moved to the outside of the crud surface. Additionally, the convective heat transfer term will be applied to the crud surface node. In this case, an equation is created for the crud node and added to the radial equation system.

Adding the crud layer presented a new challenge in that the CTF source always assumed that the outer-most node was the clad surface. For example, if the code needed the inside clad surface temperature, it would ask for the temperature at `imax-1`, where `imax` represented the outermost radial node of the fuel rod. Adding an additional radial node to the fuel rod invalidates this assumption. Therefore, it was necessary to sort through the code and assure that any sections attempting to access rod data were obtaining the correct data in the event a crud layer existed.

To prevent this type of problem in the future, the fuel rod geometry data class in CTF was modified by adding new attributes that represent specific locations of interest inside the nuclear fuel rod (i.e. pellet surface node, clad inside surface node, clad outside surface node, and crud layer surface node). These attributes will be set to the correct value during initialization of the fuel

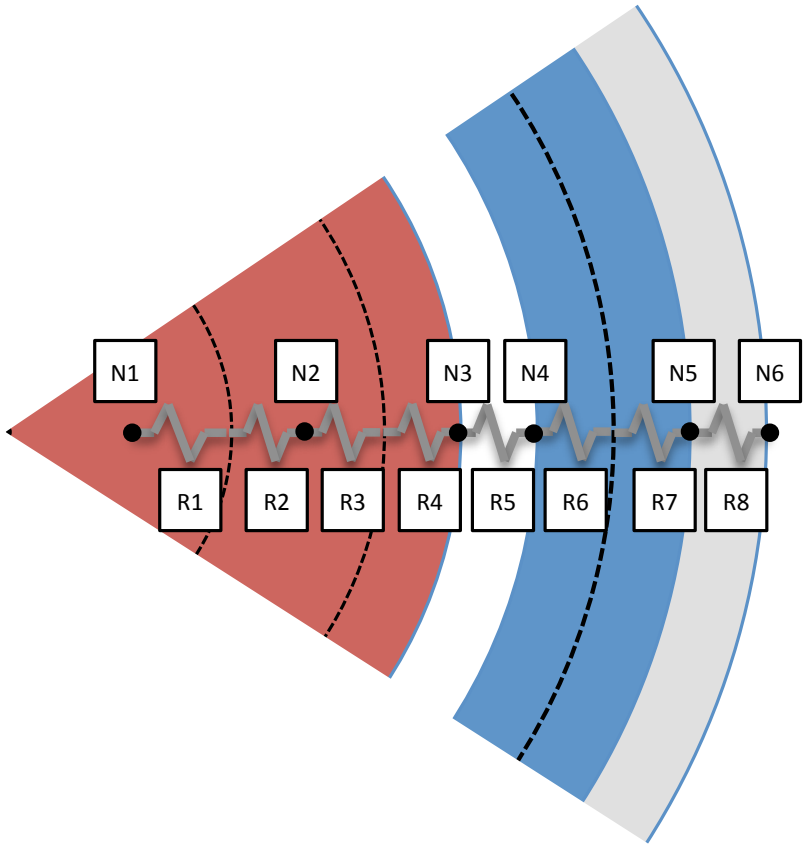

Figure 5: CTF model for fuel rods as a thermal resistance network

rod data class. Furthermore, their values were made private and accessible only by helper routines that are capable of checking if the request is being made by an actual nuclear fuel rod in order to prevent invalid usage. After making these modifications, the code was converted to obtain all fuel rod data using these accessors, ensuring that the code was getting the correct rod data after the addition of a crud layer.

6 Feature Testing

This section includes a series of demonstrations of the newly implemented reactor cycle simulation and crud growth capability that has been implemented into CTF. At this early stage of development, where only a surrogate has been developed and used to model crud growth, no validation testing has been attempted. Rather, we look to demonstrate that the feature is functioning as we would generally expect. In other words, we expect to see the following phenomena:

1. crud should form only where subcooled boiling is present,
2. thicker crud deposits should result in increased internal rod temperatures,
3. reduced crud thermal conductivity should result in higher internal rod temperatures,
4. crud should grow in a linear fashion with respect to time when core boundary conditions remain constant, and
5. rods with the highest boiling rates should have the thickest crud deposits at the end of a cycle simulation.

The following subsections seek to verify that these behaviors are observed using the new feature.

6.1 Thermal feedback verification

Section 5 presented the approach that was used to model the crud layer in the CTF rod conduction equations. This section seeks to verify that the implementation was done correctly in the source code by comparing the code result to a hand calculation. A simple single nuclear fuel rod model was created with arbitrary flow conditions and rod power. The case was run for 12 months broken into 3 month states with all operating conditions being held constant throughout the entire cycle simulation. A single surface of the rod was analyzed in this study.

This CTF model was run to steady state, so the arbitrary flow conditions will result in some wall temperature, T_w, existing at the surface of the crud. We look to use this wall temperature and the analytical formulation of crud thermal resistance to calculate the expected temperature of the outside surface of the clad. Using Figure 4 as an example, we want to determine the temperature at

CASL-U-2014-0188-000

Table 1: crud conductivity verification study results

State (months)	crud thickness (microns)	R_{crud} ($\times 10^5$ K-m/W)	$T_{\text{clad,calc}}$ (C)	$T_{\text{clad,CTF}}$ (C)
0	0.00	0.00	347.43	347.43
3	40.62	9.04	348.78	348.78
6	80.95	17.9	350.11	350.11
9	120.91	26.7	351.41	351.41
12	160.59	35.3	352.69	352.69

Node 5 knowing the temperature at Node 6 and the thermal resistance from Node 5 to 6. This simple thermal resistance network can be represented in equation form as:

$$q' = \frac{T_5 - T_6}{R_{\text{crud}}} \tag{15}$$

The linear heat rate at the rod level under consideration is q', T_5 and T_6 are the temperatures at Nodes 5 and 6, and R_{crud} is the linear thermal resistance across the crud layer, which is defined in the following equation:

$$R = \frac{\ln\left(\frac{r_6}{r_5}\right)}{2\pi k} \tag{16}$$

In this equation, r_5 and r_6 are the radii at Nodes 5 and 6 and k is the thermal conductivity of the crud. The radius at Node 5 was a constant throughout the cycle simulation, as it is the radius of the outside of the clad. The radius at Node 6, however, changed at each state of the cycle. As described in Section 4, a simplifying assumption of the crud surrogate is that the crud thermal conductivity, k, is a constant value of 15 W/m-K. With this information, we can fully define the thermal resistance at each state in the cycle. Using this in Equation 15 along with known rod surface temperature and linear heat rate, we can obtain the predicted value for clad surface temperature. Table 1 shows the results of this calculation, as well as the actual CTF results, for the 12 month cycle simulation.

The results demonstrate that the increase in crud thickness over the cycle is linear, which verifies Phenomena 4 in the list of expectations preceding this section. The results also show that thickening of the crud layer results in higher thermal resistance and, thus, higher clad surface temperatures, which verifies Phenomena 2 in the list of expectations. Furthermore, the results show that CTF predictions of clad outside temperature match the hand calculations precisely, which verifies correct implementation of the crud layer conduction equation.

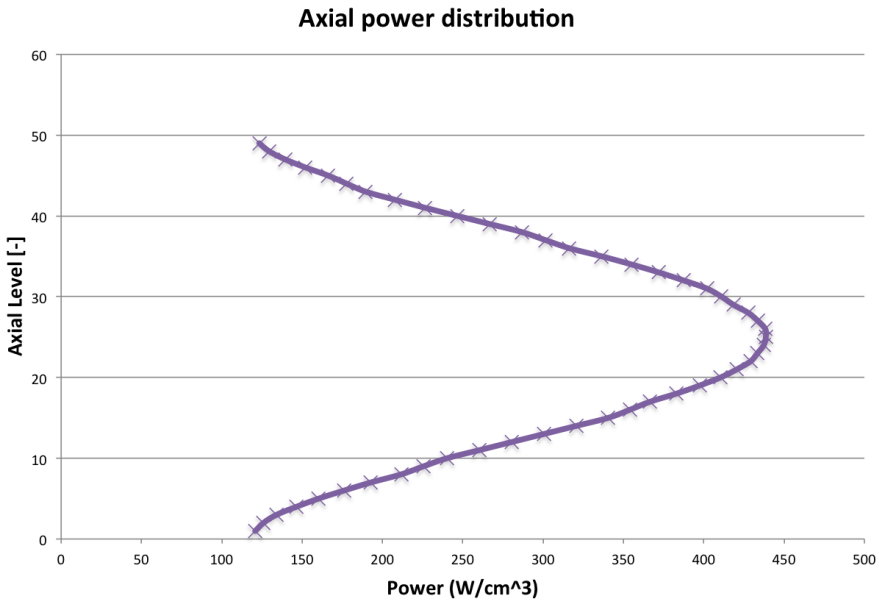

Figure 6: Axial power distribution in the nuclear fuel rod

6.2 Single rod study

For this case, a single nuclear fuel rod was modeled, discretized into 49 axial mesh cells, and with a cosine power profile applied. The case was run for 12 months with each state broken into 3 month intervals. The study was designed such that no operating conditions or rod powers were varied throughout the study.

Boundary conditions included a 0.25 kg/s inlet mass flow rate, a 292.8 C inlet temperature, and a 15.513 MPa outlet pressure. The axial power distribution in the rod for the study is shown in Figure 6. Boundary conditions were selected such that subcooled boiling occurred over a sufficient amount of the fuel rod.

Running the study for 5 state points (0, 3, 6, 9, and 12 months) leads to the five crud thickness axial profiles shown in Figure 7. In this figure, the x-axis shows the thickness of the crud in microns while the y-axis shows the rod axial mesh cell level. Results are shown for one azimuthal segment of the rod, only; however, since this case is symmetric, the crud thickness and thermal hydraulic conditions were identical for the other three rod segments. Finally, the horizontal orange line in the figure shows the axial location where additional data will be extracted from the simulation.

This figure shows that there is no crud on the rod at State 0 (red line), as we should expect. The crud becomes thicker at each successive state in the cycle. We also make note of the grid effect on crud growth; improved convective

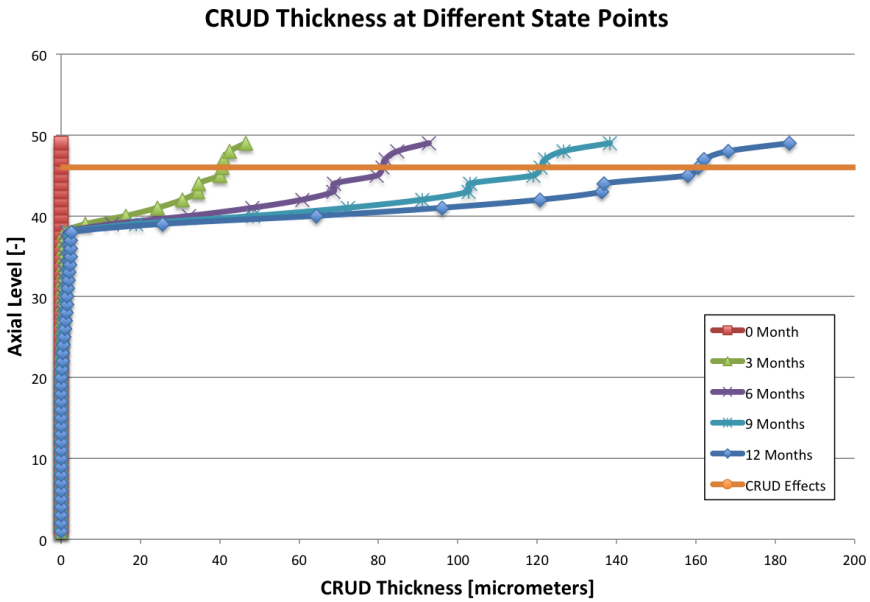

Figure 7: Axial crud thickness profiles at four state points in depletion study

heat transfer downstream of the grid reduces the steaming rate and, therefore, reduces crud growth. The trend in the linear steaming rate can be seen in Figure 8. Furthermore, we can see that there is no crud formation where the steaming rate is zero, which verifies Phenomena 1 from the list of expectations.

This figure shows that the crud thickness profile matches the steaming rate with one exception being the upper-most level of the rod. The steaming rate is highest at the N-1 level, whereas the crud thickness is highest at the N level, with N representing the top axial level in the fuel rod. This behavior is expected and can be explained by looking back to how crud thickness is defined in the surrogate using Equation 10. The deposited mass at Level N-1 is about 20% larger than the value at Level N, which matches the behavior in the steaming rate. However, the length, L, at Level N-1 is about 30% larger than the length at Level N, which results in a smaller thickness of crud growing on the Level N-1 surface. In other words, the mass of crud deposited at Level N-1 is spread over a larger surface area, which results in the thickest crud forming at the top of the rod.

Since the boundary conditions are kept constant throughout the multi-state simulation, we expect that the crud should buildup in a linear fashion with respect to time. Figure 9 shows the crud thickness at four points in the multi-state transient for a single axial level of the rod (the orange line in Figure 7). The behavior of the crud growth is linear, as expected.

Finally, we look to prove that Phenomena 3 in the list of expectations is

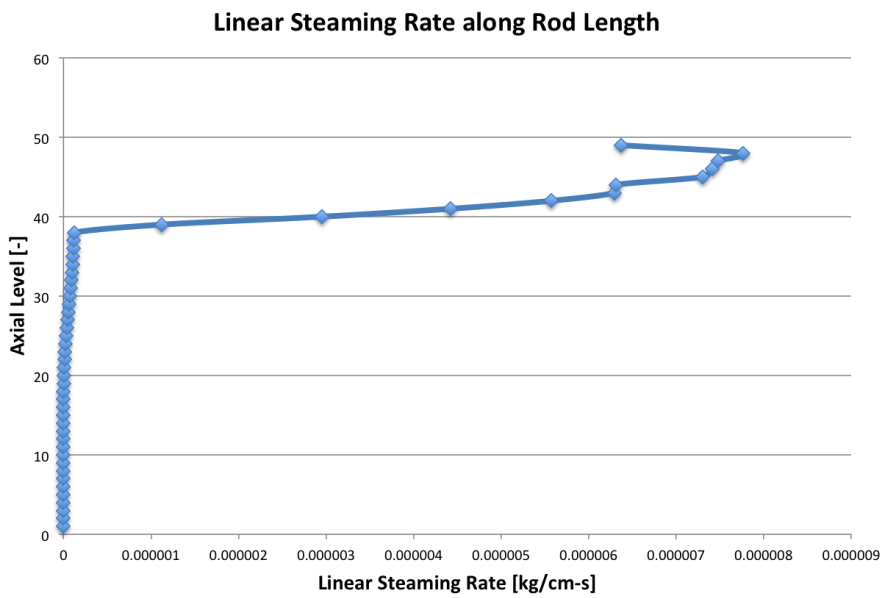

Figure 8: Linear steaming rate along the axis of the rod

correctly predicted by this new feature by reducing the thermal conductivity of the crud from 15 to 5 W/m-K and re-running this simulation. Doing this and plotting the difference in volumetric fuel temperature for the different crud thermal conductivities results in the expected behavior. This is shown in Figure 10. The additional case of no crud is included in the figure as a sanity check, showing that the volumetric averaged fuel temperature is constant throughout the cycle transient.

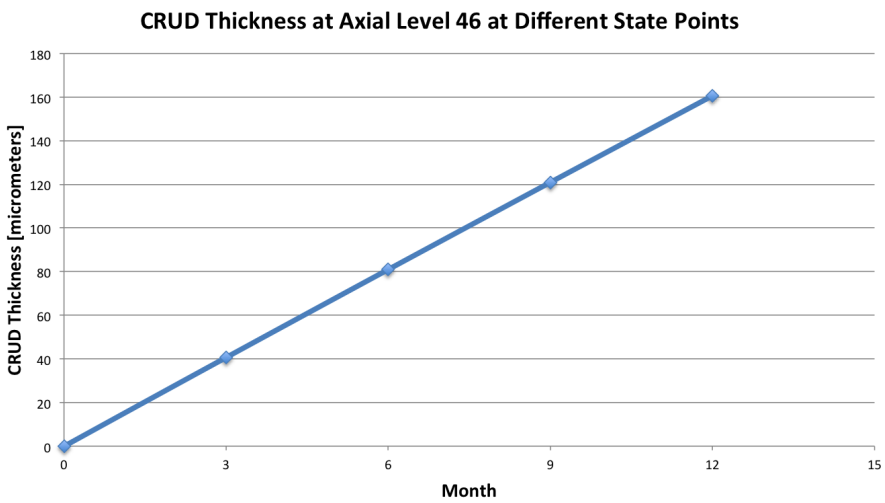

Figure 9: Growth of crud through multi-state simulation as J=46 level of fuel rod

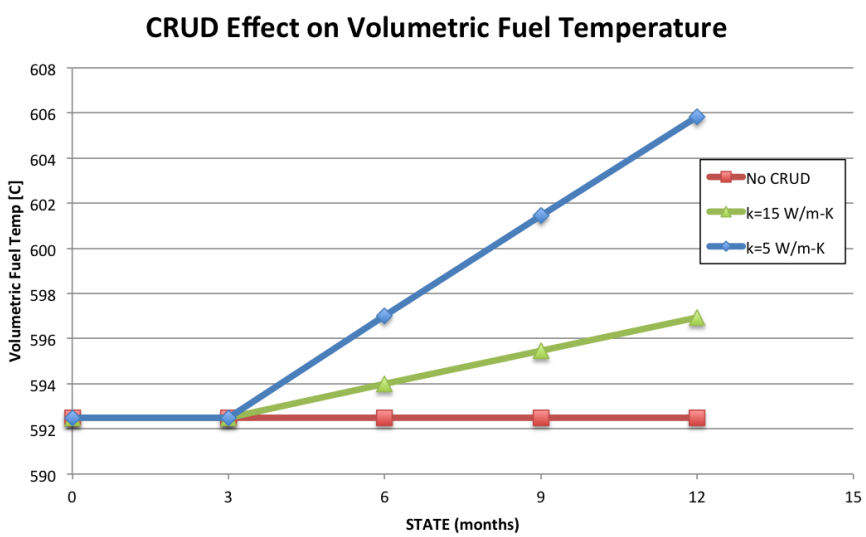

Figure 10: Effect of crud thermal conductivity on the volumetric average fuel pellet temperature

6.3 Full assembly study

In order to demonstrate that the cycle simulation crud modeling feature scales up to larger problems, a single Hot Full Power (HFP) 17x17 assembly (CASL Progression Problem 6[3]) was modeled over a cycle of 12 months. The power distribution was obtained from a coupled CTF-Denovo simulation of the problem, run to steady-state for the initial set of boundary conditions at State 1; the coupled CTF-Denovo simulation was not run at each state in the cycle. Instead, the initial power distribution obtained for State 1 was used throughout the entire reactor cycle simulation. The cycle was started with boundary conditions matching the Problem 6 problem specification, but inlet temperature was increased throughout the cycle in order to promote steaming and, consequently, crud growth in the assembly. Table 2 provides the boundary conditions applied during the cycle.

One change was made to the power distribution obtained from the CTF-Denovo simulation; the power of one fuel pin was increased by 20% over its nominal value in order to better demonstrate that the location with the maximum steaming rate will have the maximum crud growth. An isometric view of the rod bundle is shown in Figure 11. In the figure, the surface heat flux is being visualized. This figure indicates that the maximum power is experienced in the center of the fuel assembly.

To see the interior of the bundle, where heat flux is at its highest, a threshold filter was applied to this figure in order to make lower powered rods translucent. This filtered image is shown in Figure 12. With the filter applied, the rod in which the power was increased by 20% becomes visible. A top view of the assembly, taken at the middle axial level where power is highest, is shown in Figure 13. This figure shows that the fuel rod at Row 14, Column 7, has a significantly higher power than any other rod in the assembly at that axial level.

Next, we look to observe the rod steaming characteristics in the assembly. Note that the bundle power distribution was constant throughout the 12-month cycle that was modeled; however, because the inlet temperature was increased at successive state points, the steaming rate in the bundle increased throughout the cycle. Figure 14 shows an isometric view of the bundle with rod surface

[3]Document to reference for Problem 6 specification?

Table 2: Boundary conditions for single HFP assembly 12 month cycle

State (month)	Inlet Temperature (C)	Inlet Mass Flow Rate (kg/s)	Outlet Pressure (MPa)
0	292.8	85.98	15.5132
3	295.8	85.98	15.5132
6	298.8	85.98	15.5132
9	298.8	85.98	15.5132
12	299.8	85.98	15.5132

steaming rate being visualized. This visualization was produced at the end of the operation cycle, so it represents maximum bundle steaming. Note that a threshold filter was applied to facilitate viewing steaming inside the bundle. From the figure, we can see that the steaming is occurring downstream of the location where maximum bundle power occurs. Furthermore, we also see that more steaming occurs on the hot rod. To better show this, this image was zoomed-in, which is shown in Figure 15.

Figure 16 was generated in order to show the correspondence between steaming rate and bundle void content. It shows an isometric view of the top of the rod bundle, where steaming is occurring. The lower portion of the figure shows the fuel rods with the steaming rate being visualized using a purple-to-pink color scheme. In the upper portion of the assembly, the channel void content is visualized using a translucent rainbow color scheme. This figure shows void content increasing downstream of the steaming locations. Note how void content increases around the hot rod before steaming starts on any other fuel rods in the assembly. Even after steaming stops, void continues to travel up and out the top of the bundle. At the top of the bundle, we can also see maximum void content at the location of the hot rod.

Next, we look at the effect of this steaming rate on crud growth. Since steaming occurs at the top of the bundle, we focus the visualizations at that location. Figure 17 shows the crud thickness on the rod surfaces at the beginning of the cycle. This images shows all rods as translucent, which means there is zero crud throughout the bundle. After 3 months of operation, crud starts to form in the locations with highest steaming rates. This is shown in Figure 18. The hot rod accumulates the thickest deposits, which verifies Phenomena 5 in the list of expected observations that was presented at the beginning of this section. Figures 19 and 20 show the crud thickness at 6 months and the end of the cycle, respectively. The crud deposits mimic the rod steaming distribution throughout the bundle.

Finally, we look to demonstrate the effect of the crud layer on the fuel rod thermal solution in CTF by comparing clad surface temperature with and without crud. To do this, a second cycle simulation was run with the crud surrogate turned off. The operating conditions were kept identical to those of the first study. The clad surface temperature in the crud deposit region of the bundle was visualized with and without the crud model turned on. The first image, Figure 21, shows an isometric view of the upper portion of the bundle with clad surface temperature being visualized. A threshold filter was applied to show the interior region of the bundle. Note that the legend scale goes from 345 to 375 Celsius. When the crud model is turned off, no clad surface temperatures exceed 347 Celsius. Next, Figure 22 shows the same thing as Figure 21, but with the crud model turned on. Here, we see that the clad temperatures are clearly higher as a result of the crud deposits, going as high as 375 Celsius in the non-hot-rod fuel rods. The hot rod clad temperatures reach much higher temperatures due to a severe over-prediction of crud deposits compared to other fuel rods.

CASL-U-2014-0188-000

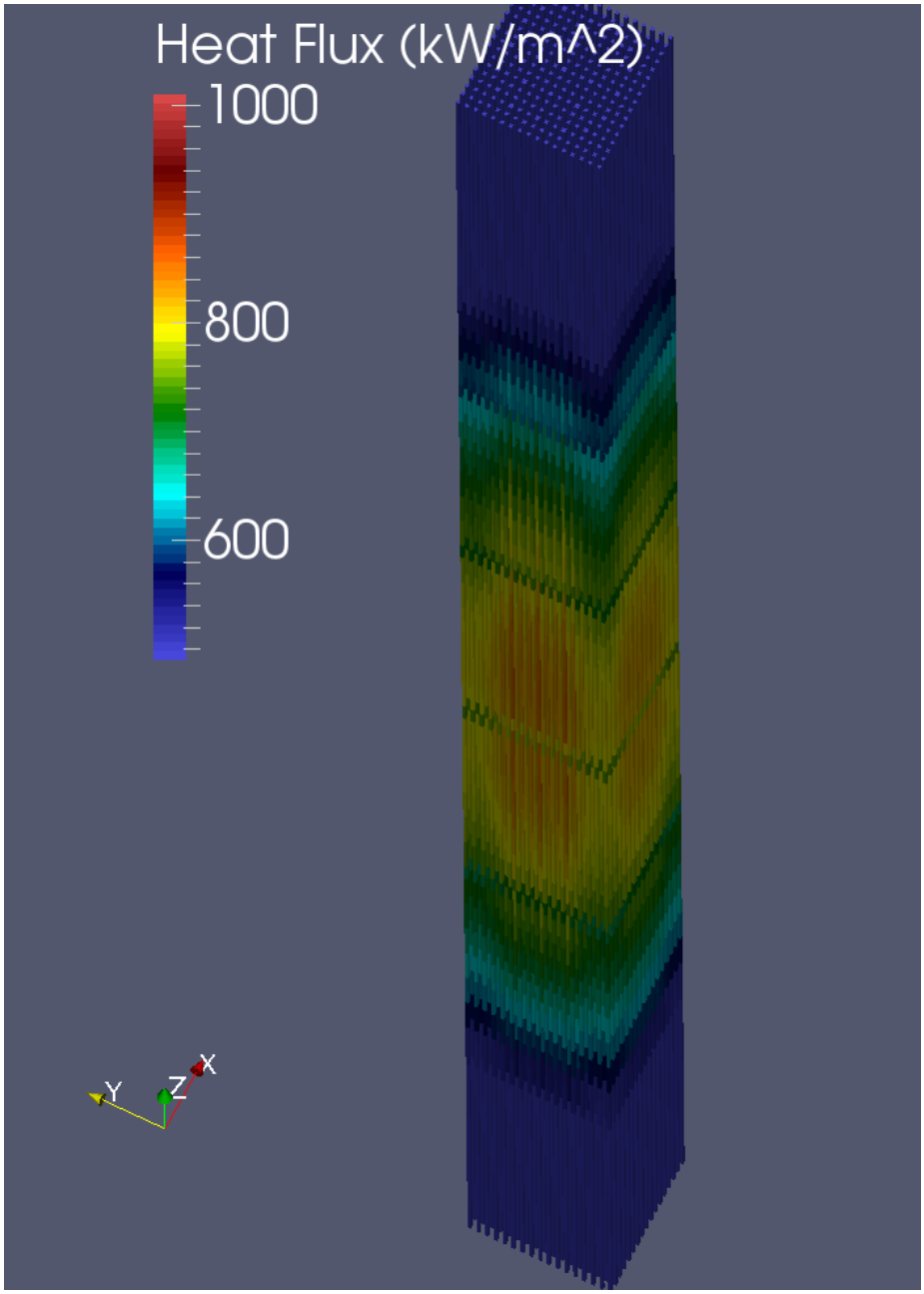

Figure 11: Rod surface heat flux in assembly throughout cycle

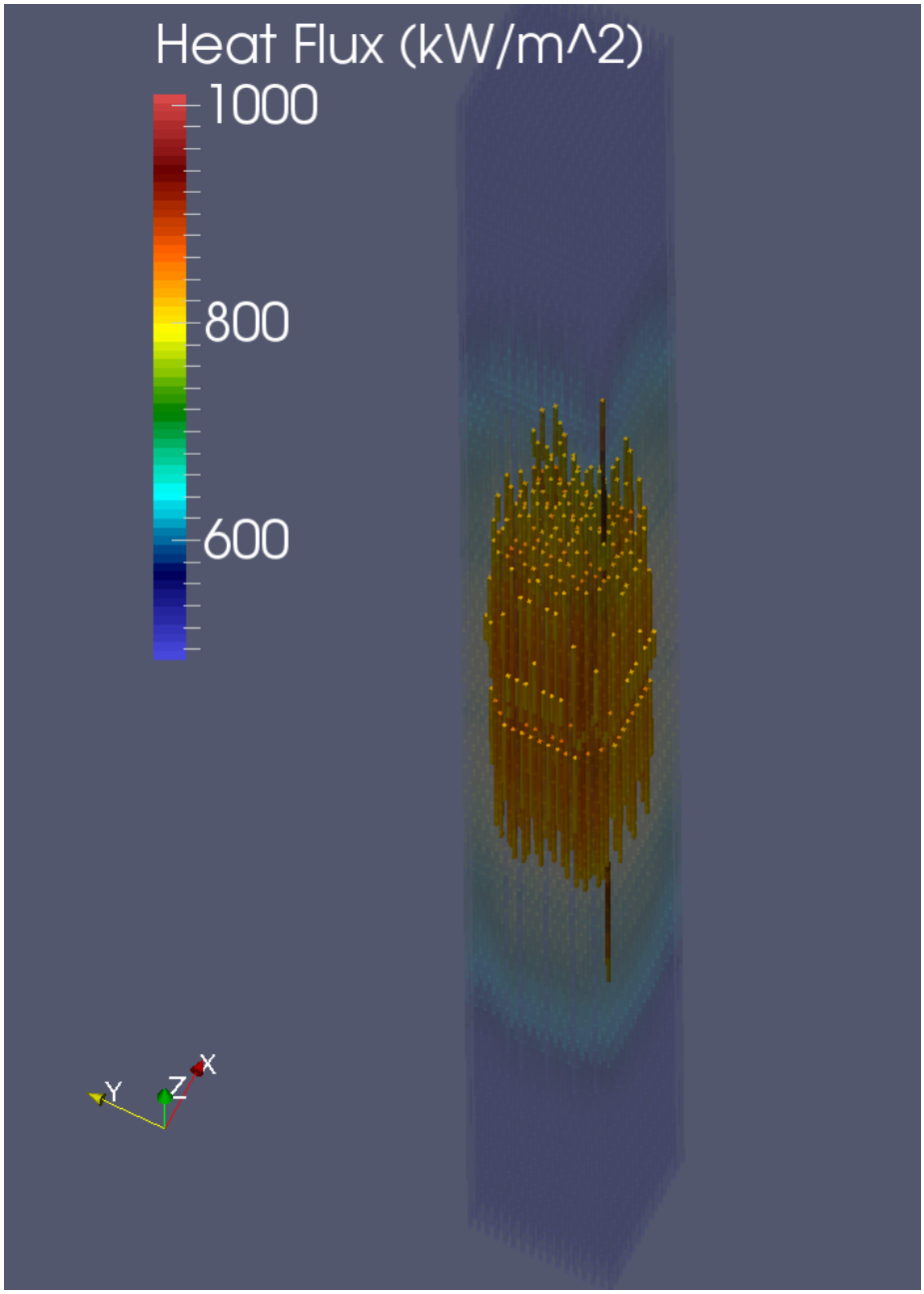

Figure 12: Rod surface heat flux in assembly throughout cycle (threshold filter applied)

CASL-U-2014-0188-000

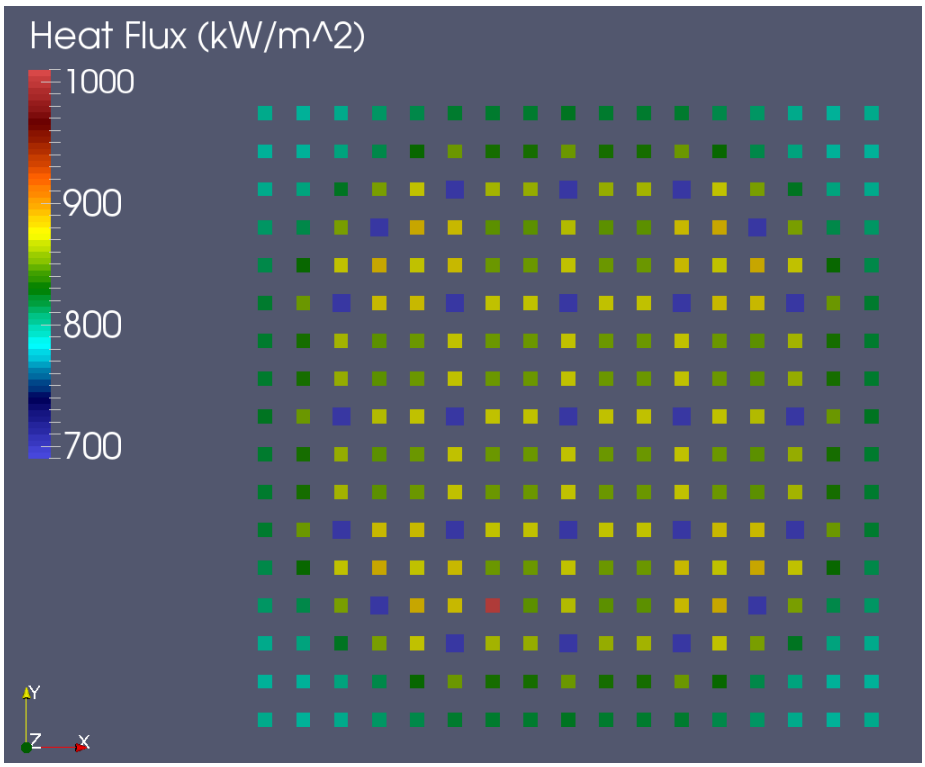

Figure 13: Top view of assembly taken at middle axial level with surface heat flux being visualized

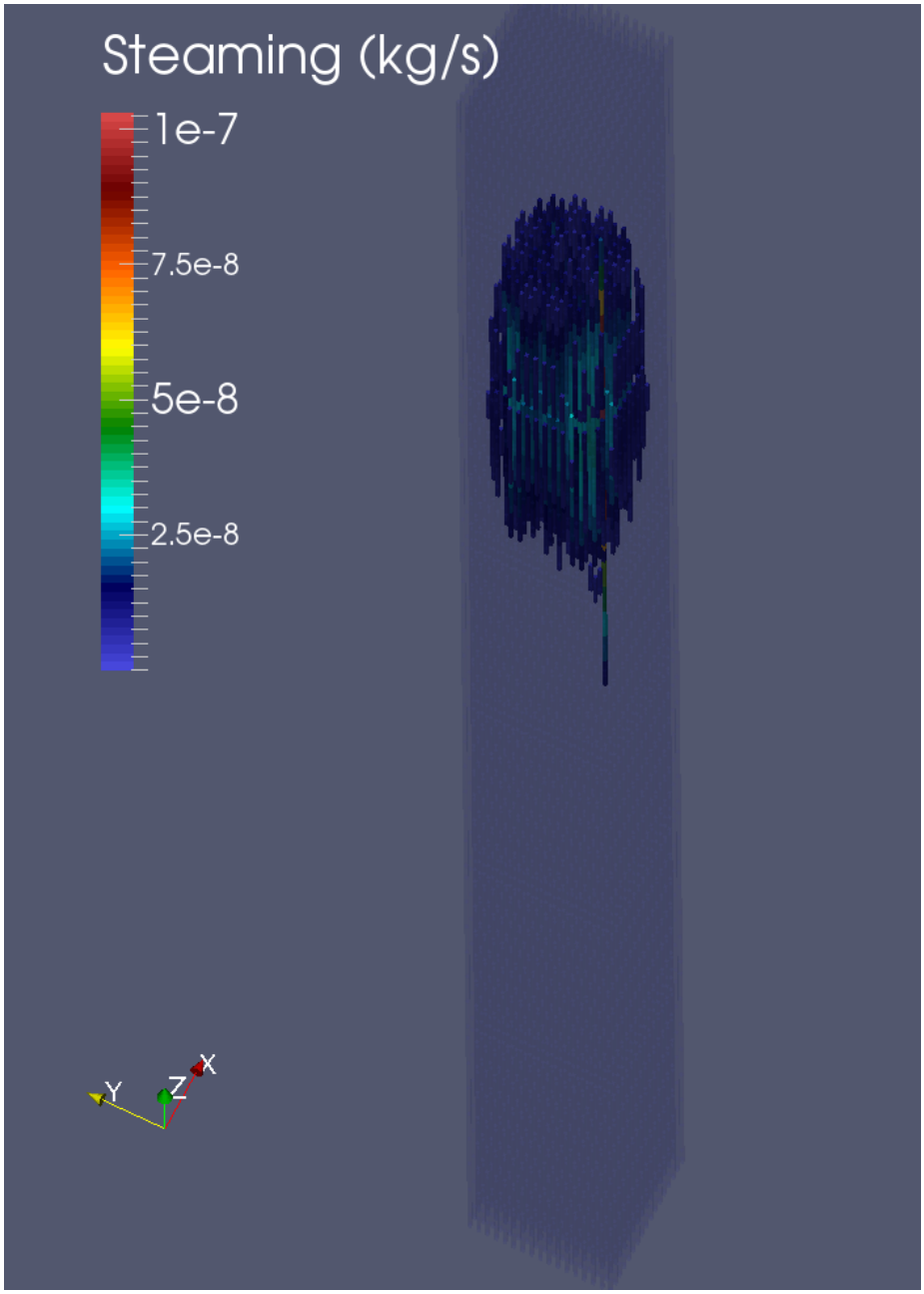

Figure 14: Isometric view of assembly with steaming rate at end of cycle visualized

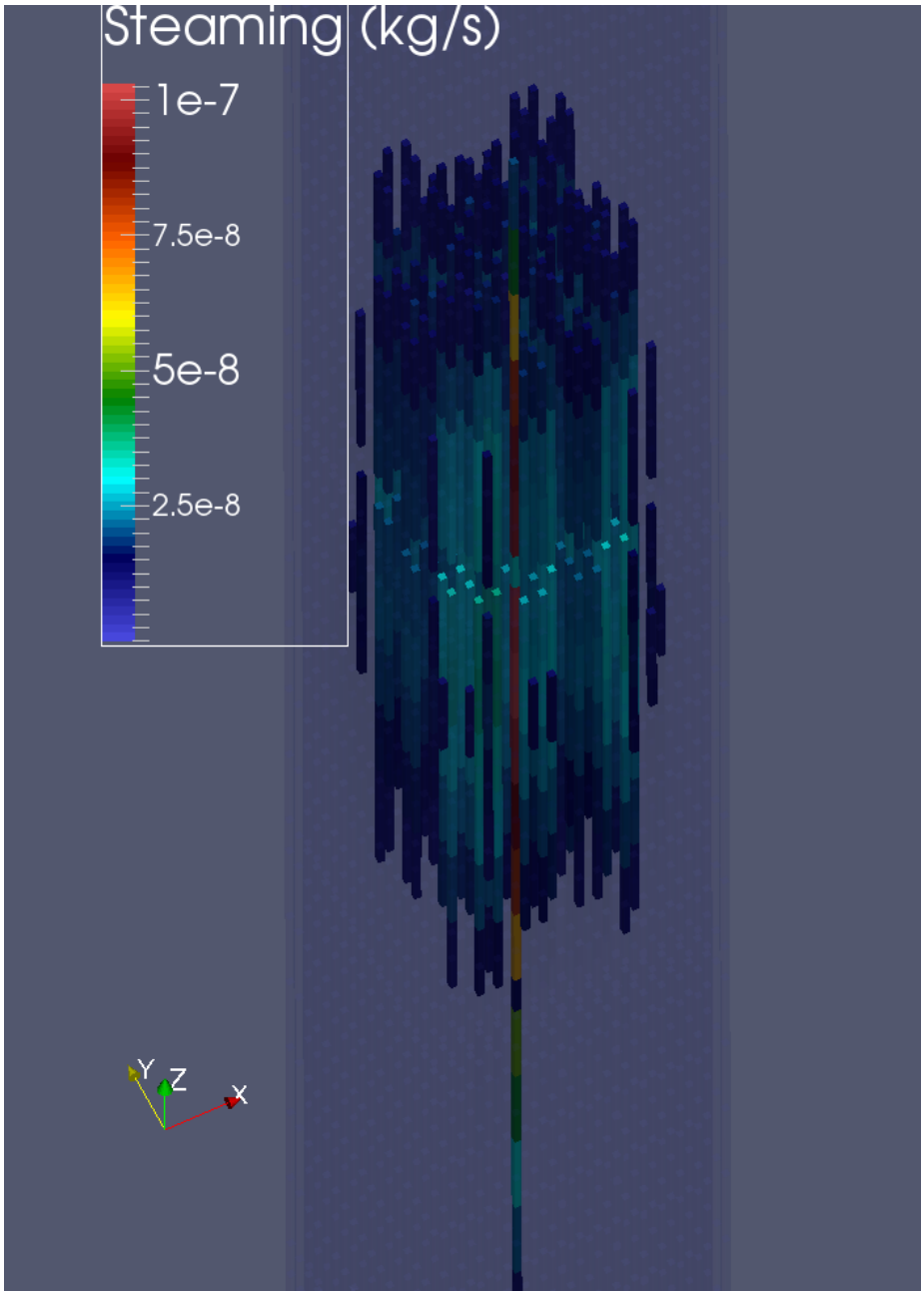

Figure 15: Isometric view of assembly with steaming rate at end of cycle zoomed to steaming location

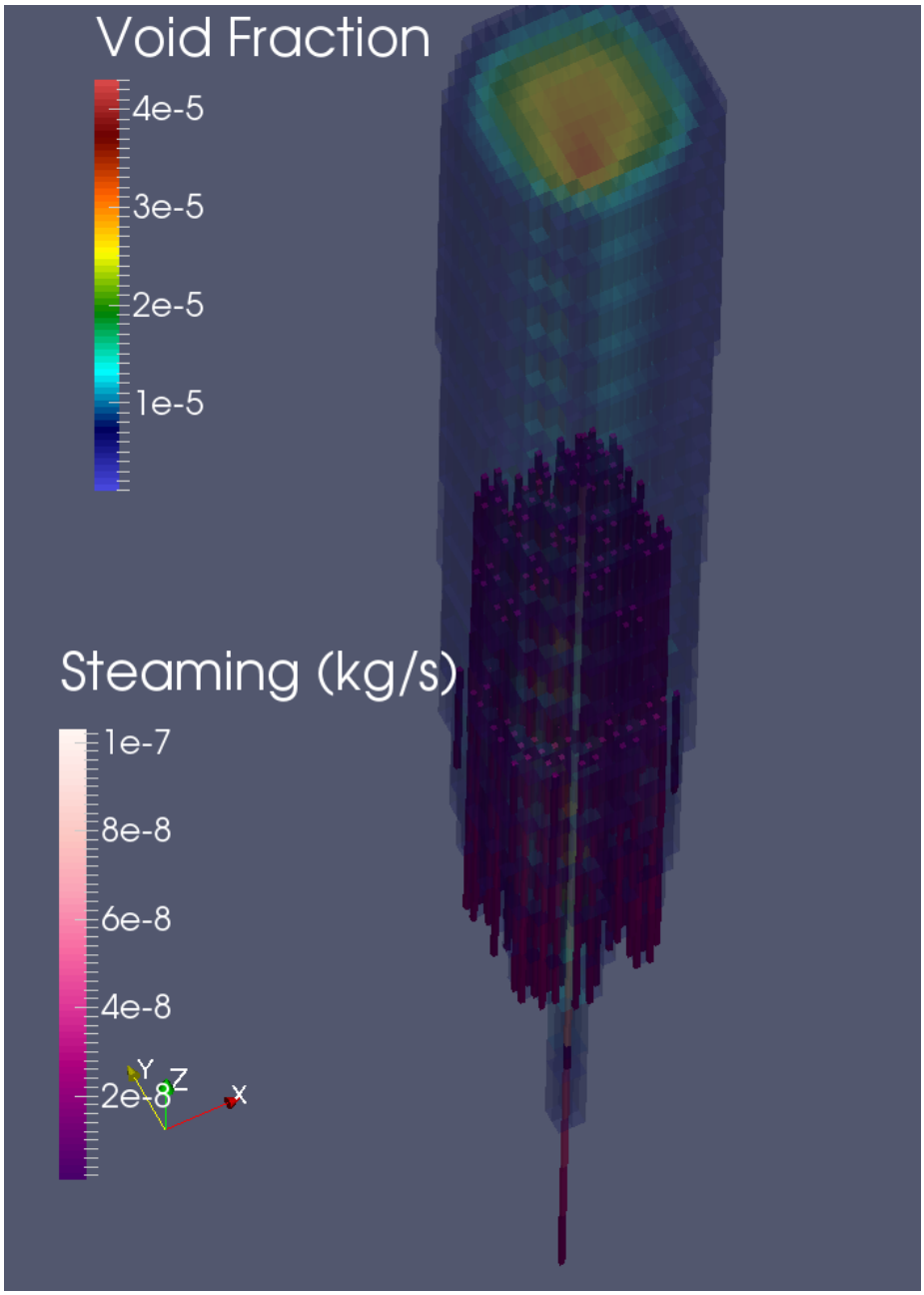

Figure 16: Isometric view of assembly at steaming location with rod steaming (pink color scheme) and channel void (translucent rainbow color scheme) being visualized

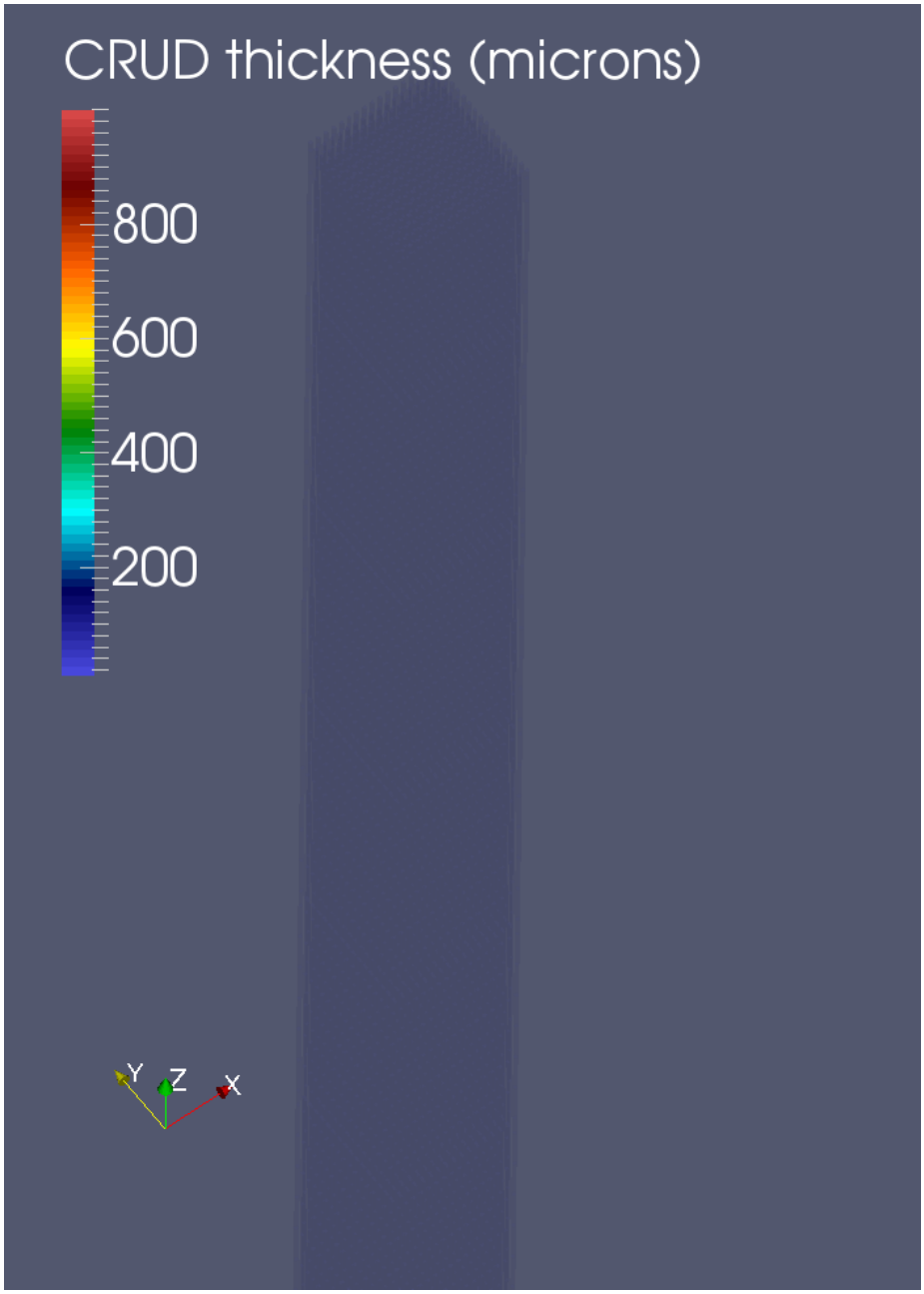

Figure 17: Crud thickness in assembly at beginning of cycle

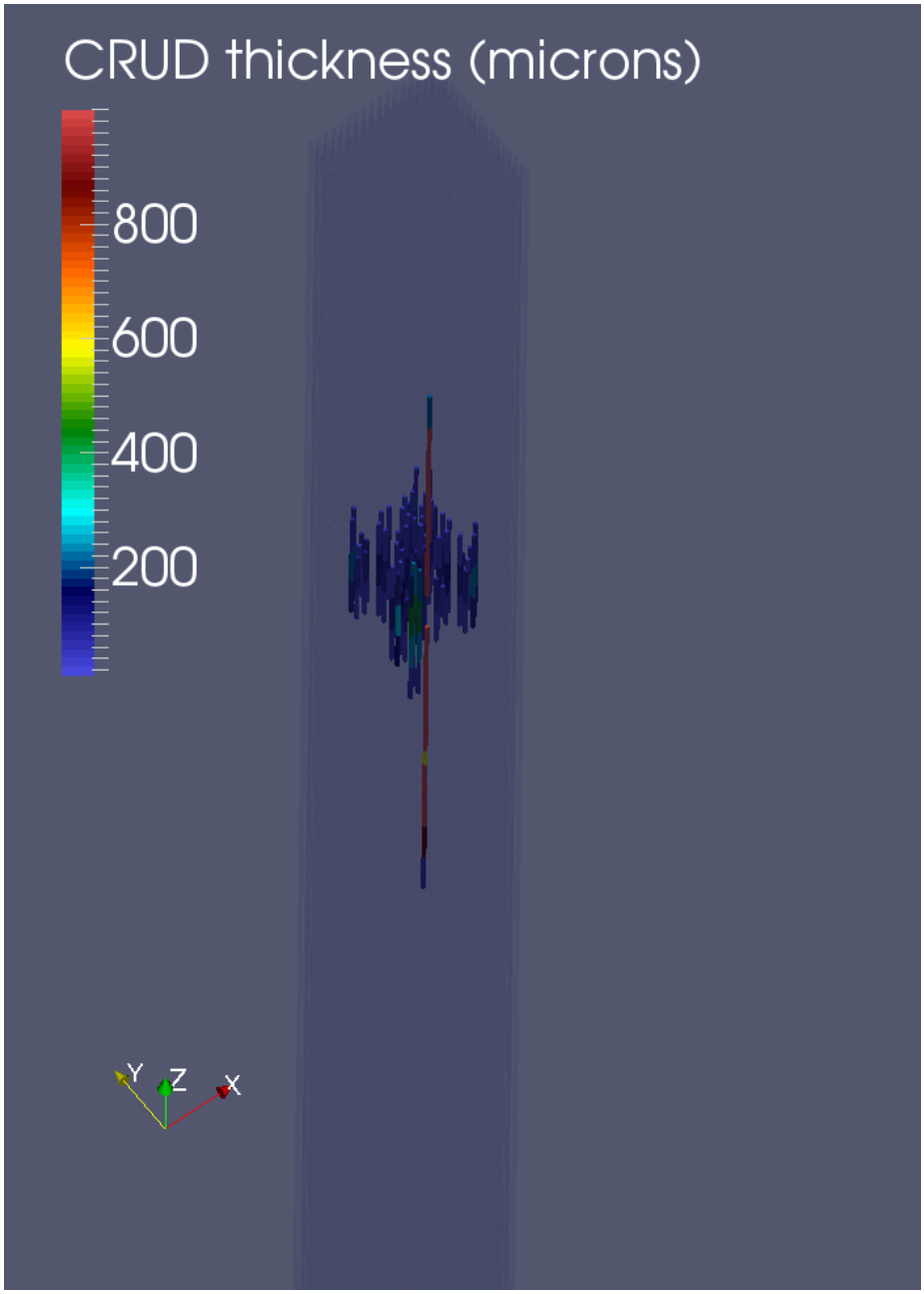

Figure 18: Crud thickness in assembly at 3 months into cycle

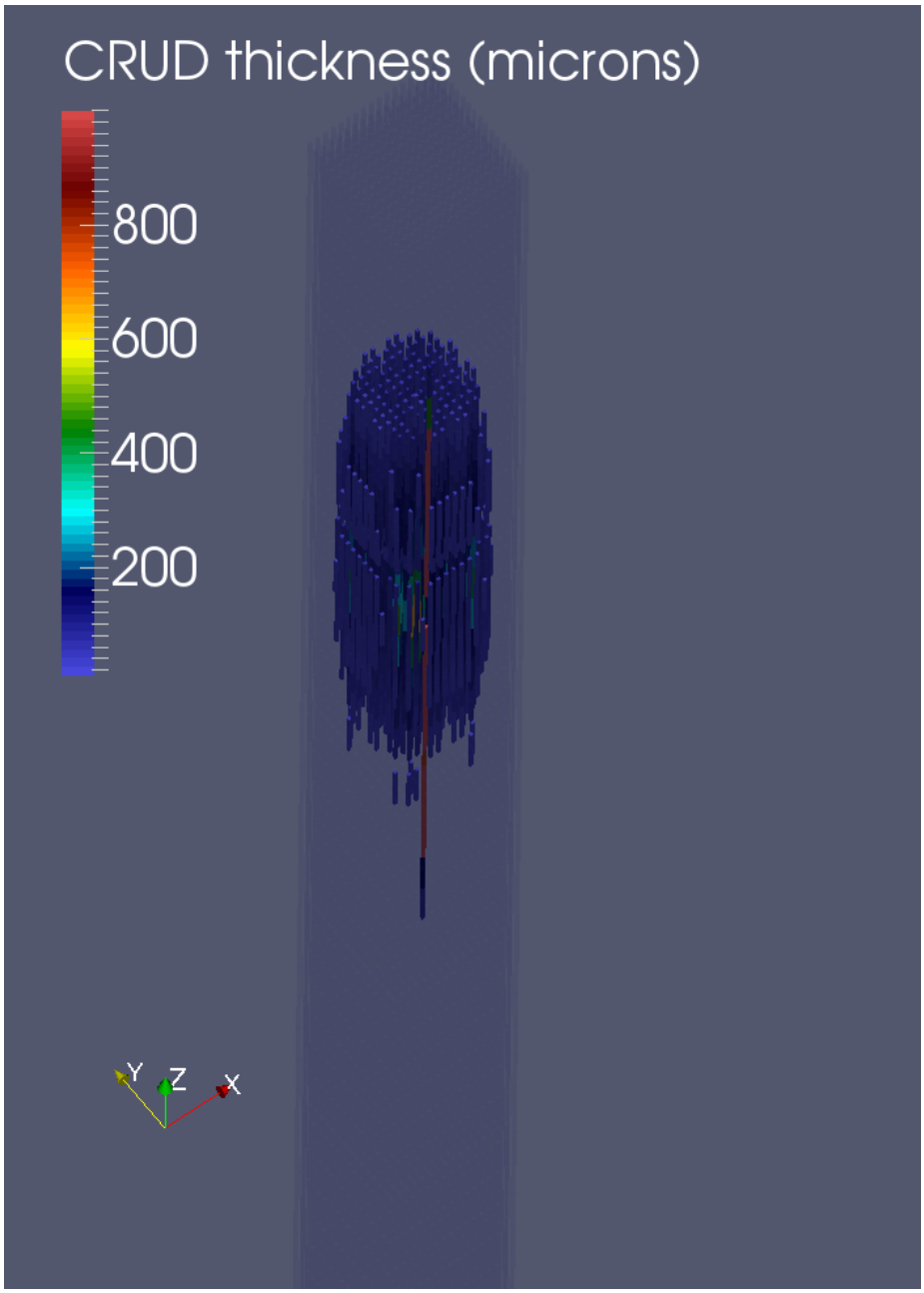

Figure 19: Crud thickness in assembly at 6 months into cycle

CASL-U-2014-0188-000

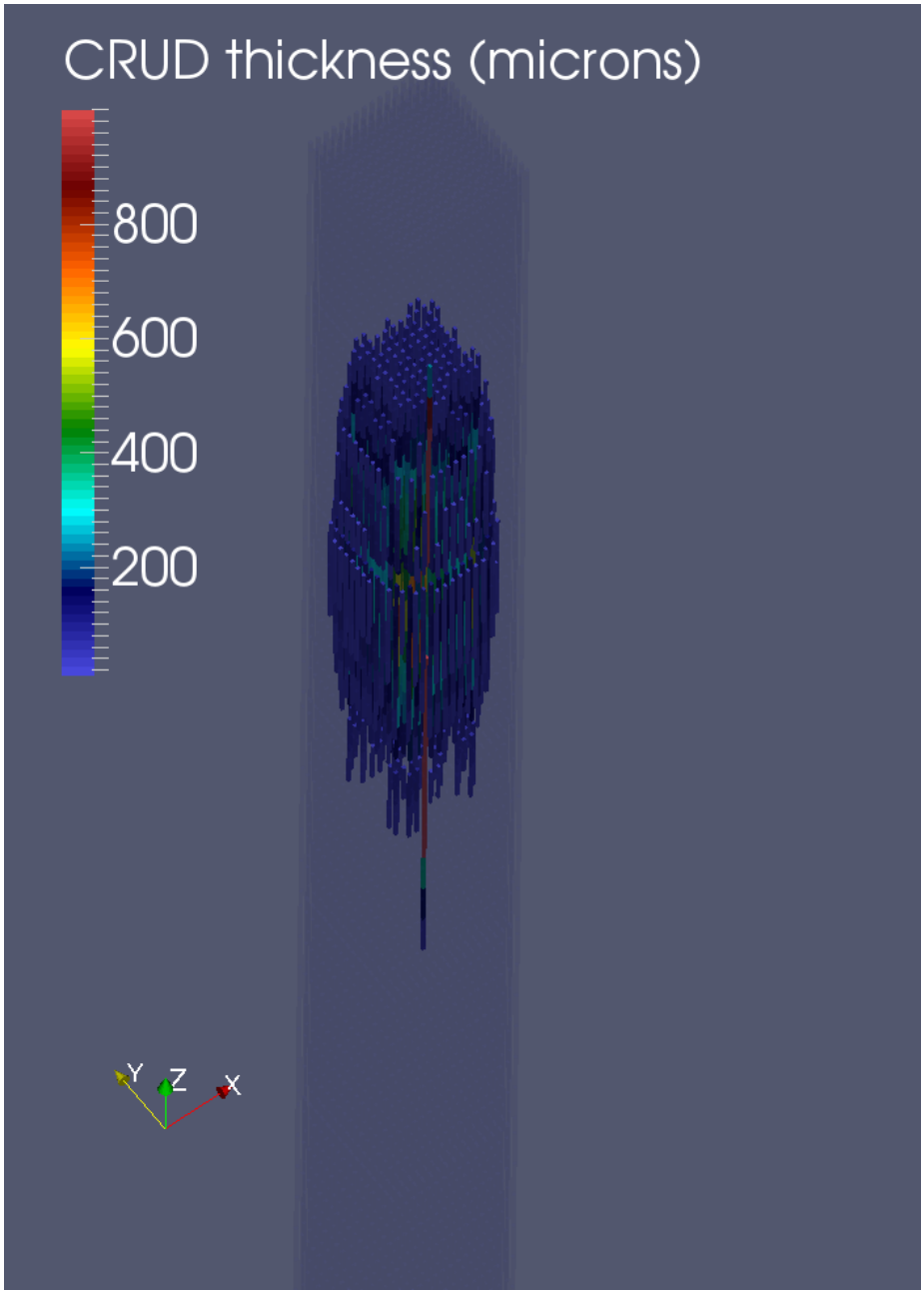

Figure 20: Crud thickness in assembly at end of cycle

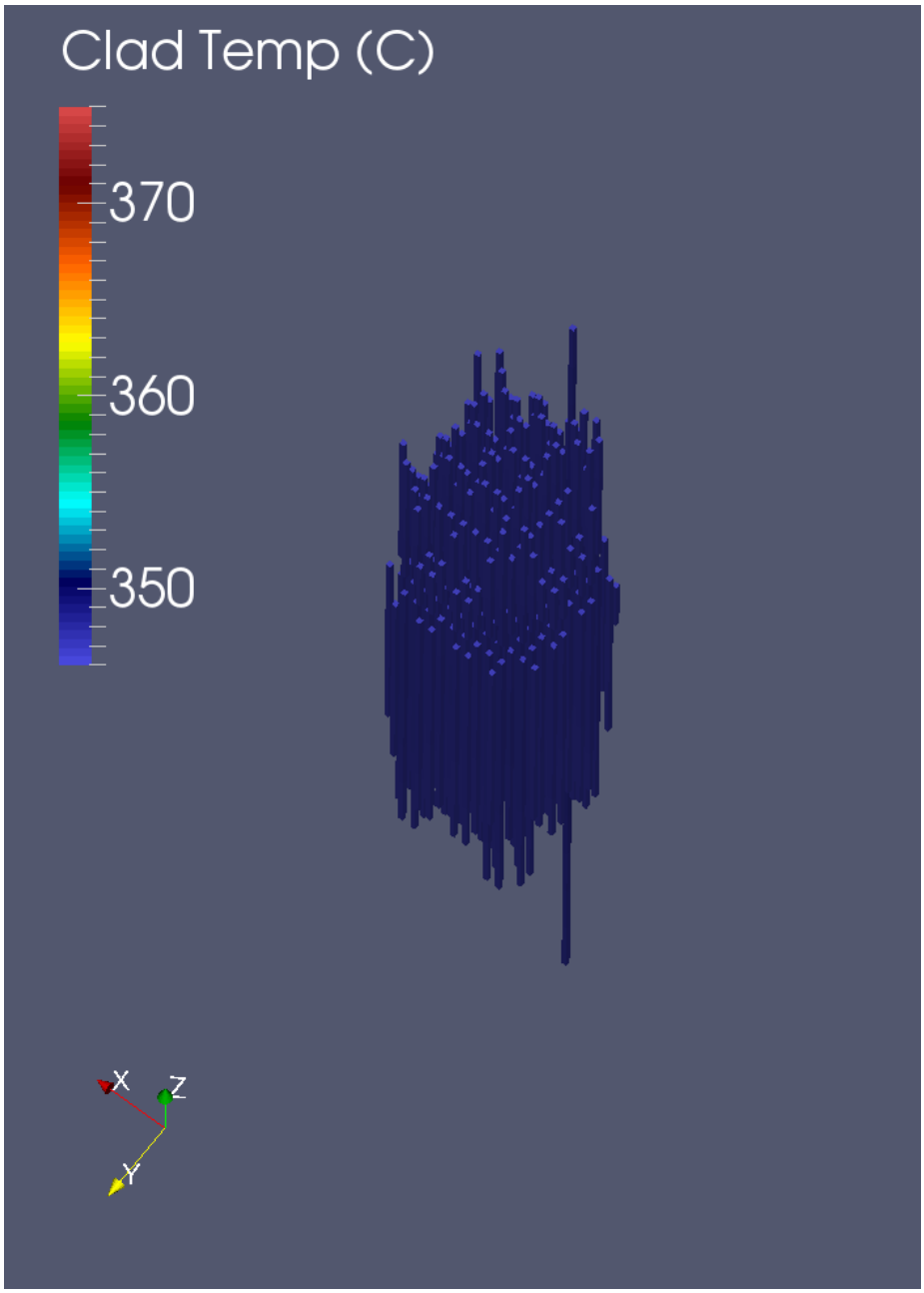

Figure 21: Clad surface temperature in upper bundle at end of cycle with crud model deactivated

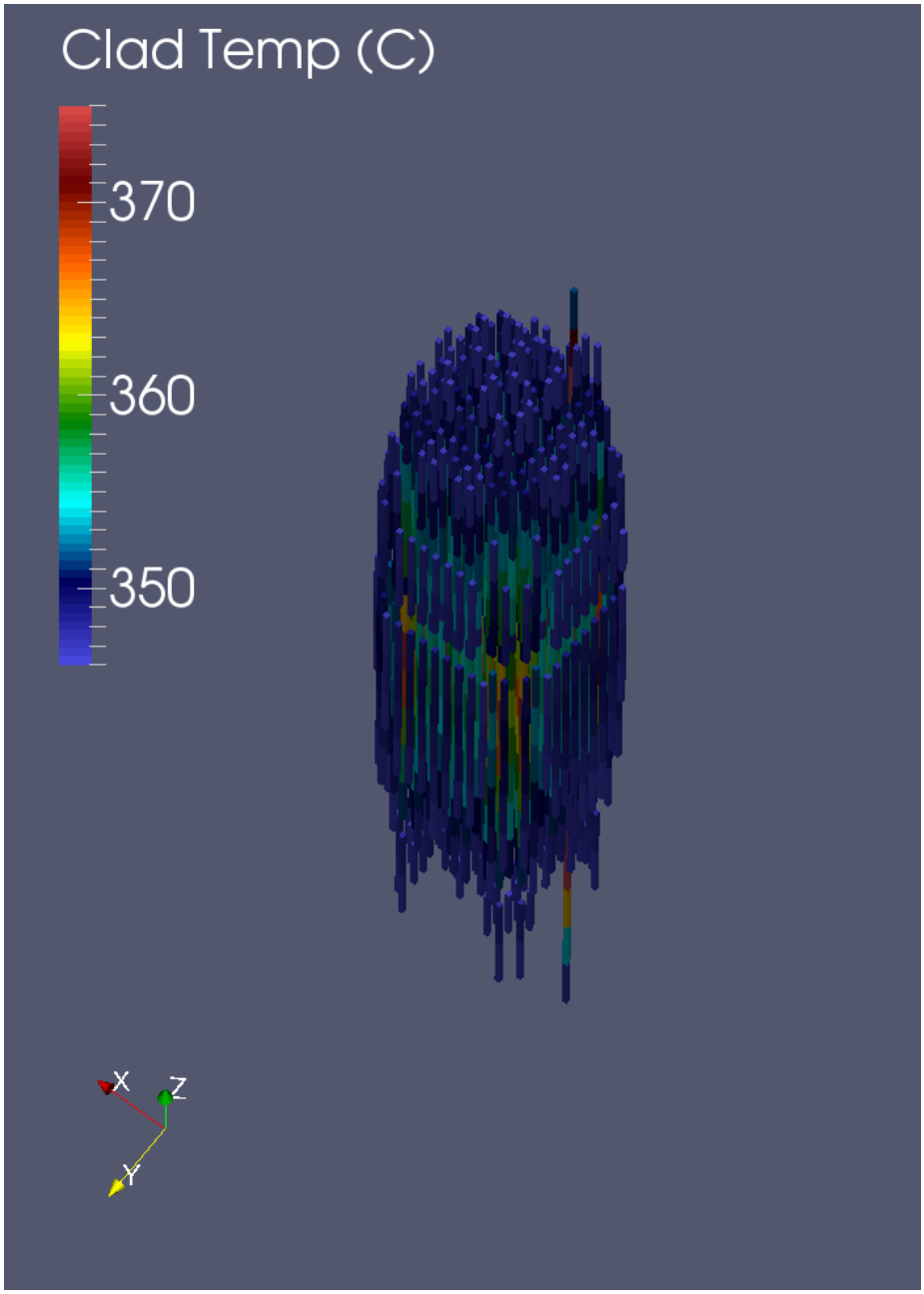

Figure 22: Clad surface temperature in upper bundle at end of cycle with crud model activated

7 Conclusion

This report documents the development and implementation of a capability to model reactor operation cycles with crud growth in the CTF thermal hydraulic subchannel code. Creating this capability required the completion of several tasks, including: developing a CTF driver program, creating a coupling interface to CTF, developing a crud surrogate utility, expanding the code HDF5 capabilities to read in detailed core power distributions, and modifying the CTF rod solution to include the thermal impact of the crud layer. These tasks have been completed, resulting in a crud modeling capability in CTF.

Verification work has been performed and presented to demonstrate basic proper functioning of the new capability and that the crud thermal feedback feature has been correctly implemented. Additionally, the feature was demonstrated to properly scale up to a full 17x17 assembly model and behave as expected.

While preliminary verification work has been presented, no validation activities have been undertaken. Future work should focus on implementing more physically realistic models into the crud surrogate and comparing results to actual measurements. Furthermore, the work done as part of this milestone has laid a foundation for coupling to more physically realistic crud modeling capabilities in the future.

Acronyms

CASL Consortium for Advanced Simulation of Light water reactors

CILC Crud-Induced Localized Corrosion

CIPS Crud-Induced Power Shift

crud Chalk River Unidentified Deposits

CTF Pennsylvania State University version of COBRA-TF

EPRI Electric Power Research Institute

HDF5 Hierarchal Data Format 5

LHS Left-Hand Side

PWR Pressurized Water Reactor

RHS Right-Hand Side

RR Release Rate

SS Stainless Steel

VERA Virtual Environment for Reactor Applications

VERA-CS Virtual Environment for Reactor Applications—Core Simulator

References

[1] L. Zou, H. Zhang, J. Gehin, and B. Kochunas. Coupled Thermal-Hydraulic/Neutronics/CRUD Framework in Prediction of CRUD-Induced Power Shift Phenomenon. *Nuclear Technology*, 183, 2013.

[2] J. Deshon, D. Hussey, B. Kendrick, J. McGurk, J. Secker, and M. Short. Pressurized Water Reactor Fuel Crud and Corrosion Modeling. *JOM*, 63(8), August 2011.

[3] R.K. Salko and M.N. Avramova. *CTF Theory Manual*. The Pennsylvania State University.

[4] M.N. Avramova. CTF—A Thermal-Hydraulic Sub-Channel Code for LWR Transient Analyses—User's Manual. Technical report, The Reactor Dynamics Fuel Management Group at the Pennsylvania State University, 2009.

[5] A. Godfrey, S. Palmtag, G. Davidson, and B. Collins. Veraout—vera hdf5 output specification. Technical report, Oak Ridge National Laboratory, 2014.

[6] S. Sawochka. Impact of PWR Primary Chemistry on Corrosion Product Deposition on Fuel Cladding Surfaces. Technical Report TR-108783, EPRI, 1997.

CASL-U-2014-0188-000